Journal of Great Lakes Research 41 (2015) 818–829

Contents lists available at ScienceDirect

Journal of Great Lakes Research

journal homepage: www.elsevier.com/locate/jglr

Dynamic internal drivers of a historically severe cyanobacteria bloom in Lake Champlain revealed through comprehensive monitoring

Peter D.F. Isles [a,b,*], Courtney D. Giles [b], Trevor A. Gearhart [b,c], Yaoyang Xu [b], Greg K. Druschel [b,d], Andrew W. Schroth [b,e]

[a] Rubenstein School of Environment and Natural Resources, University of Vermont, Aiken Center, 81 Carrigan Drive, Burlington, VT 05405, USA
[b] Vermont EPSCoR, University of Vermont, Cook Physical Science Building, 82 University Place, Burlington, VT 05405, USA
[c] Department of Biology, University of Vermont, Rm. 120A Marsh Life Sciences, 109 Carrigan Drive, Burlington, VT 05405, USA
[d] Department of Earth Sciences, Indiana University Purdue University Indianapolis, 723 W. Michigan Street, SL118, Indianapolis, IN 46202, USA
[e] Department of Geology, University of Vermont, Delehanty Hall, 180 Colchester Ave., Burlington, VT 05405, USA

ARTICLE INFO

Article history:
Received 6 March 2015
Accepted 18 June 2015
Available online 10 July 2015

Communicated by R. Michael McKay

Index words:
Cyanobacteria bloom
Internal phosphorus loading
Lake Champlain
Resource limitation
High-frequency data

ABSTRACT

The shallow bays of Lake Champlain have experienced increasingly severe algal blooms over recent decades, but the drivers of inter- and intra-annual variability of bloom severity are poorly understood. Disentangling the relative importance of multiple processes driving cyanobacteria blooms is difficult, in part because traditional monitoring programs often lack adequate temporal resolution, and in part because many studies seek to identify a single dominant mechanism. In this study, a holistic approach was used to identify multiple drivers of a strong cyanobacterial bloom over time in a shallow, eutrophic bay of Lake Champlain utilizing high-temporal-resolution meteorological, water quality, and biogeochemical sensor data; an intensive field sampling program; and a long-term monitoring dataset. In contrast to studies in similar systems, spring runoff and nutrient loads could not explain the severity of the 2012 bloom. Instead, internal nutrient loading and hydrodynamic conditions mediated shifts in resource limitation. The cyanobacteria growth phase was associated with the depletion of available nitrogen and sediment phosphorus release. The peak bloom stage was characterized by multiple limiting resources and stable water column conditions. The decline phase of the bloom was associated with light limitation brought about by wind mixing, and was punctuated by a major storm event, which brought a major biogeochemical shift in the lake system. This study illustrates the complexity of cyanobacteria resource limitation in response to internal and external forcing over time, and also the power of comprehensive monitoring approaches in disentangling complex drivers of eutrophic ecosystem function that vary across temporal and spatial scales.

Introduction

Cyanobacteria blooms in the northeastern arm of Lake Champlain (Vermont and New York, USA; Quebec, Canada) have increased over the past 50 years (Smeltzer et al., 2012), particularly in the shallow, eutrophic bays. This mirrors a global increase in the occurrence of toxic and nuisance cyanobacteria blooms in recent decades resulting from land use changes and climate warming (Dokulil and Teubner, 2000; Paerl and Huisman, 2009). Shallow lakes and bays are particularly sensitive to these stressors because factors such as large ratios of catchment area to lake volume, relatively warm temperatures and the accessibility of benthic nutrients may all predispose them to cyanobacterial dominance (Søndergaard et al., 2003). There is general consensus that inputs of nutrients are the most important long-term driver of increases in blooms, as well as the most practical target of management interventions (Schindler, 2012; V. H. Smith and Schindler, 2009); however, the effects of changes in the temporal patterns of nutrient inputs are incompletely understood (Vanni et al., 2006), and nutrient effects may be mediated by the effects of physical drivers (Huisman et al., 1999, 2004) or food web structure (Carpenter et al., 1985; Jeppesen et al., 1997).

Recent research has focused on the importance of winter and spring nutrient inputs in driving phytoplankton dynamics during the bloom season (Gerten and Adrian, 2000; Pierson et al., 2013). Strong positive correlations have been identified between spring river discharge (as well as spring inputs of total phosphorus and reactive phosphorus) and the magnitude of summer cyanobacteria blooms in western Lake Erie (Michalak et al., 2013; Stumpf et al., 2012). Lake Champlain lies within the same geographic region as the Laurentian Great Lakes and shares many of their geological, physical and ecological characteristics (Facey et al., 2012), suggesting that algae blooms in Lake Champlain may be controlled by similar factors. In addition to the effects of spring runoff, external river inputs during the summer growing season may

* Corresponding author at: Rubenstein Ecosystem Science Laboratory, University of Vermont, 3 College st., Burlington VT 05401, USA. Tel.: +1 802 338 8250.
E-mail addresses: peter.isles@uvm.edu (P.D.F. Isles), Courtney.Giles@hutton.ac.uk (C.D. Giles), trevor.gearhart@uvm.edu (T.A. Gearhart), yaoyang.xu@uvm.edu (Y. Xu), gdrusche@iupui.edu (G.K. Druschel), andrew.schroth@uvm.edu (A.W. Schroth).

http://dx.doi.org/10.1016/j.jglr.2015.06.006
0380-1330/

have complex effects on lake phytoplankton dynamics at varying timescales dependent on the antecedent nutrient and phytoplankton conditions in the receiving waters and the degree to which discharge events are accompanied by lake mixing (Jennings et al., 2012).

The paradigm of phosphorus (P) as the key nutrient limiting production in lakes has guided research and management for several decades and has resulted in significant improvements in water quality in many systems (Litke, 1999; Schindler, 1977); however, recent papers highlighting the importance of co-limitation by nitrogen (N) and P have produced renewed interests in the role of N limitation at ecologically meaningful timescales (Scott and McCarthy, 2010; Sterner, 2008). In western Lake Erie, recent research has found evidence for N limitation in late summer cyanobacteria blooms (Chaffin et al., 2013). This echoes findings from lakes in Germany, which have found increasing incidence of N-limitation late in the summer (Kolzau et al., 2014).

The timing of internal nutrient processing may vary greatly between lakes, and can dramatically alter water column nutrient stoichiometry (Søndergaard et al., 2005). The mechanisms that control the release of benthic P are fairly straightforward in stratified lakes with hypoxic hypolimnia, where the reductive dissolution of iron and manganese oxyhydroxides leads to the release of adsorbed P to the water column. The mechanisms are more complex in shallow systems where thermal stratification occurs periodically or not at all and where oxygen is typically abundant throughout the water column, but where high fluxes of sediment P are observed nonetheless (Hupfer and Lewandowski, 2008; Jensen and Andersen, 1992; Søndergaard et al., 1999). In these systems, benthic P release may be driven by reducing conditions resulting from temporary hypoxia during periods of transient thermal stratification (Burger et al., 2008), or by other factors such as high pH (Boers, 1991; Jin et al., 2006; Seitzinger, 1991) or nitrate (Jensen and Andersen, 1992). In addition to differences in P cycling, N transformations also differ between shallow and deep waters. Warmer sediment temperatures and complete water column mixing may accelerate denitrification in shallow bays relative to deeper systems (McCarthy et al., 2013; Van Luijn et al., 1999), and shallow bays may have increased availability of reduced inorganic N due to the breakdown of organic N compounds in the sediments or through dissimilatory or assimilatory nitrate reduction when oxygen is absent (Burgin and Hamilton, 2007). Nitrogen fixation may also be important to the nitrogen budget of both deep and shallow lakes, and the magnitude of N fixation may vary in response to multiple factors, particularly ammonium concentration (Muro-Pastor et al., 2005).

The multiple internal and external mechanisms that impact the balance of N and P suggest that the factors driving this balance may operate at multiple temporal scales. Some processes such as photosynthesis-driven shifts in dissolved oxygen occur at short temporal scales (hourly to daily) (Staehr et al., 2011), some processes such as wind mixing or peaks in river discharge are episodic and may cause rapid ecosystem responses when they do occur (Jennings et al., 2012), some such as denitrification or diagenesis of detrital nutrients occur gradually on seasonal scales, and some such as anthropogenic nutrient inputs and climate changes are the result of both multi-annual trends and seasonal patterns (Piña-Ochoa and Álvarez-Cobelas, 2006; Reitzel et al., 2012). This multiplicity of scales may help to explain divergent interpretations of basic ecosystem processes, because these interpretations may vary greatly depending on measurement intervals (Carpenter and Kitchell, 1987; Levin, 1992; McGill, 2010).

The advent of automated sensor technology in combination with long-term monitoring data and robust field sampling programs has the potential to address incongruities in interpretations of trends in resource limitation which arise from processes operating at multiple timescales (D. M. Anderson et al., 2012). High-frequency sensors enable researchers to observe rapid ecosystem shifts in response to episodic events and to identify drivers of physical and biological processes that cannot be resolved using the weekly or bi-weekly data produced by traditional monitoring programs. In this study, we use data from an automated monitoring platform moored in a temperate shallow eutrophic bay in combination with an intensive field-sampling program and long-term monitoring data to 1) assess the severity of the 2012 bloom in Missisquoi Bay relative to other years; 2) assess the importance of external nutrient and water inputs in driving the severity of summer blooms; 3) quantitatively describe internal nutrient dynamics across the initiation, propagation, and senescence of an algal bloom; and 4) mechanistically describe the drivers of these dynamics across these stages of the bloom.

Methods

Study site

The study was conducted at a monitoring platform moored in Missisquoi Bay, Lake Champlain, which spans the border between Vermont, USA and Quebec, Canada (Fig. 1). Missisquoi Bay is eutrophic and has experienced regular blooms of toxic cyanobacteria over the past two decades composed primarily of *Microcystis* (mostly *Microcystis aeruginosa*, with smaller populations of *Microcystis wesenbergii*), *Dolichospermum* (predominantly *Dolichospermum circinalis*, *Dolichospermum flos-aquae*, and smaller populations of *Dolichospermum crassa*), and *Aphanizomenon flos-aquae* (Levine et al., 2012; Lake Champlain Long-Term Monitoring Program, http://www.watershedmanagement.vt.gov/lakes/htm/lp_longterm.htm; Angela Shambaugh, Vermont Agency of Natural Resources, 2015, *personal communication*). The bay is large (75 km^2), uniformly shallow (max depth 5 m, mean depth 2.8 m) and can be considered to be isolated hydrodynamically from the main body of Lake Champlain, the only outflow being a 200 m opening through a causeway in the southwest. Our monitoring platform was moored in the southeastern portion of the bay at N 44° 59.503′, W 73° 06.798′. Depth at the study site ranges from 3 to 4 m in 2012. The main tributary is the Missisquoi River, which accounts for 79% of total discharge into the bay (Limnotech, 2012). The Missisquoi River drains a large forested (62%) and agricultural (25%) watershed (Levine et al., 2012) which spans the US–Canada border and is heavily impacted by nonpoint source agricultural pollution (Smeltzer and Simoneau, 2008). Two other rivers, the Pike and the Rock, account for 18% and 3% of total discharge into the bay, respectively (Limnotech, 2012).

Historical water quality data

Water quality data for total phosphorus, total nitrogen, chlorophyll-*a*, and surface pH from 2006 to 2012 were obtained from the Lake Champlain Long Term Monitoring Program website (http://www.watershedmanagement.vt.gov/lakes/htm/lp_longterm.htm) for station 51 (VTDEC (Vermont Department of Environmental Conservation) and NYDEC (New York State Department of Environmental Conservation), 2014). Spatial surveys have found water quality parameters at this location to be more similar to the site of the current study than the other long-term monitoring site in Missisquoi Bay (Isles, unpublished data).

Automated data collection

Water quality and meteorological data were collected using a modified YSI vertical profiling system (YSI systems, Yellow Springs OH) equipped with a YSI 6980 Controller Assembly, a YSI 6955 Winch Assembly, a meteorological (MET) station, and a depth sounding unit. The controller assembly housed independent CR1000 dataloggers (Campbell Scientific, Logan UT, USA) for the sonde and MET stations, which were linked to a single modem via a PakBus configuration. LoggerNet Pro v. 4 software (Campbell Scientific, Logan UT, USA) was used to communicate with the winch and MET dataloggers. Power was supplied to the station by a 12 V battery, interfaced to two solar panels by solar charger/regulator.

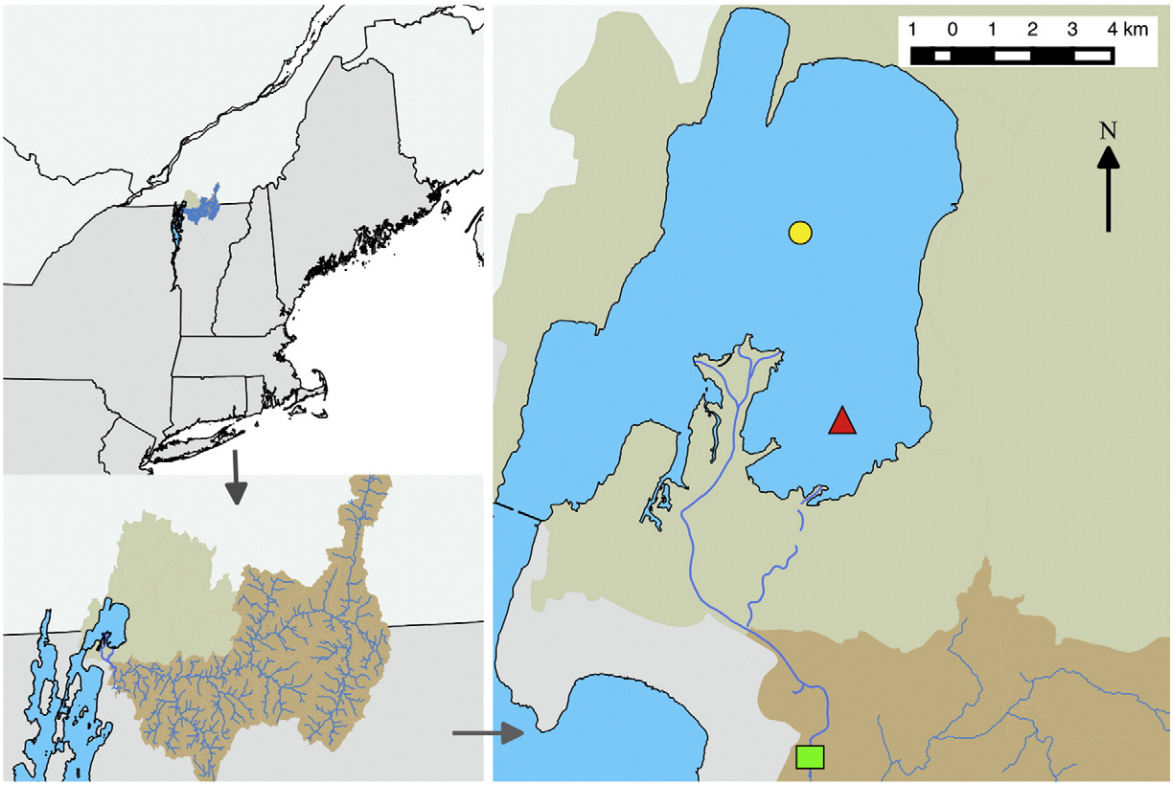

Fig. 1. Missisquoi Bay and the Missisquoi River watershed in Vermont, USA and Quebec, Canada. Missisquoi Bay long-term monitoring site indicated with circle, high-frequency data collection site indicated with triangle, and the Missisquoi River gage station is indicated with rectangle.

The winch assembly was equipped with a YSI 6600V2 sonde containing probes for temperature (°C), conductivity (mS cm^{-1}), pH, dissolved oxygen (mg L^{-1}), phycocyanin fluorescence (PC; Relative Fluorescence Units, RFU), chlorophyll-*a* fluorescence (Chl-*a*; RFU), and turbidity (nephelometric turbidity units; NTU). The sonde was calibrated weekly following the manufacturer's recommendations. Phycocyanin is a pigment specific to cyanobacteria and has been shown to be a good predictor of cyanobacteria biovolume in Missisquoi bay, while Chl-*a* measured using a YSI 6025 sensor has been shown to be a poor predictor of cyanobacteria biovolume (McQuaid et al., 2011; Zamyadi et al., 2012), and can be seen as primarily reflecting the abundance of eukaryotic phytoplankton, although there may be some contribution from phycocyanin-containing cryptophyte species. Changes in the ratio of PC to Chl-*a* can therefore be interpreted as shifts in the relative proportions of cyanobacteria and eukaryotic phytoplankton. Sonde profiles were programmed to occur hourly at 0.5 m increments throughout the water column. The bottom 1 m of the water column was excluded to prevent collision of the probes with the sediment surface during periods of high wave activity. The meteorological station included sensors for wind speed and direction, air temperature, relative humidity, pressure, and solar, as well as an internal compass to correct for buoy orientation. Meteorological data was logged at 30 min intervals. The platform was deployed on 29 June 2012 and removed for the season on 6 November 2012. Sonde and met station data collection came online on 18 July 2012.

Two ISCO automated water samplers (Teledyne ISCO, Lincoln NE) were mounted on the deck of the platform with intake hoses at 0.5 m and 2 m below the water surface and set to collect samples for total nitrogen (TN) and total phosphorus (TP) analysis every 8 h at 5:00 h, 13:00 h, and 21:00 h daily (EDT). ISCO bottles were pre-acidified using concentrated sulfuric acid (0.1%) to preserve samples for nutrient analysis and collected weekly.

Weekly field sampling and water column measurements

Weekly field sampling was conducted at the site of the automated buoy throughout the season starting on 29 June and continuing through 26 October. Duplicate water samples were collected at each of 5 depths as measured from the water surface (<0.1, 1, 2, 2.5, 3 m) using a Van Dorn bottle to capture vertical gradients of nutrients and phytoplankton within the water column. All samples were collected in 1 L acid-rinsed bottles and kept on ice for transport back to the lab. Samples for dissolved metals were collected in separate acid-washed polyethylene bottles. Photosynthetically active radiation (PAR; μmol m^{-2} s^{-1}) profiles of the water column were taken weekly at 0.5 m increments using a LI-193 spherical quantum sensor (LI-COR Biosciences, Lincoln NE).

Sample processing

Within 24 h of collection, lake and river samples (1 L) were subsampled for nutrient, metals, and phytoplankton analyses. Total N and P samples were acidified to pH < 2 (0.1% H_2SO_4) and stored at room temperature. Soluble reactive P (SRP) and dissolved inorganic N (DIN; NO_3^-/NO_2^-, NH_4^+) samples were filtered (0.45 μm PES) and stored at 4 °C (<24 h) and −20 °C, respectively. Dissolved metal samples were prepared by filtration through 0.45 μm PES followed by acidification (0.1% hydrochloric acid) and storage at room temperature. Phytoplankton samples were preserved in 1% Lugol's solution with glass beads to prevent degradation of silica in diatoms and synurophytes.

Analysis of nutrients and metals

Soluble reactive P was determined by molybdenum colorimetry with ascorbic acid modification (USEPA, 1995) using a Shimadzu 1601 UV–vis spectrophotometer (10 cm path length; Shimadzu Scientific

Instruments Corp., Columbia MD, USA). Dissolved NO_3^-/NO_2^- was measured using EPA method 353.2 (USEPA 1993a) and NH_4^+ concentrations were determined using EPA method 350.1 (USEPA, 1993b) and measured using an AQ2 Autoanalyzer (Seal Analytical, Mequon WI). Following persulfate digestion (Std. Method 4500 P-J.; APHA, 2005), total N and Total P were determined using EPA methods 353.2 and 365.1, respectively (USEPA, 1993c). Throughout this study, nutrient concentrations are reported based on elemental mass (e.g., P or N rather than PO_4^{3-} or NO_3^-), and all nutrient ratios are expressed as molar ratios. Dissolved metal concentrations as well as total dissolved phosphorus (TDP) were measured by inductively-coupled-plasma-mass-spectroscopy (ICP-MS; Element 2, Thermo Scientific) at the Woods Hole Oceanographic Plasma Facility. The protocols of Shiller (2003) were followed for dissolved trace metal sampling.

Phytoplankton samples

Surface phytoplankton biovolume was measured using the FlowCAM© imaging-in-flow system (Fluid Imaging Technologies, Yarmouth, ME). All samples were imaged in autoimage mode at 200×, 100×, and 40× magnification. 40× magnification was found to be sufficient to estimate >90% of total biovolume during the bloom, and was used to quantify large and colonial phytoplankton >25 μm in diameter (measured as areal-based diameter, ABD). These estimates did not capture populations of small unicellular phytoplankton, which may make up a majority of total biovolume during some non-bloom periods. FlowCAM estimates have been found to provide similar results to microscope counts, particularly with respect to the relative proportions of different groups (Álvarez et al., 2013). A subset of samples was counted using the Utermöhl inverted microscope technique for validation of FlowCAM estimates, and FlowCAM-estimated cyanobacteria biovolume was also compared to sonde phycocyanin estimates (Electronic supplementary material (ESM) Fig. S1). All microscope counts were conducted at 400×, and all counts contained at least 100 grids or 100 natural units of the most abundant phytoplankton species. Species identifications followed Prescott (1962; 1978), Wehr and Sheath (2002), and Komarek and Zapomelova (2007), with considerable assistance from the online key Phycokey (Baker et al., 2012). Additional net phytoplankton cell count and biovolume data were acquired from the Lake Champlain Long-Term Monitoring Program for station 51 (VT DEC and NY DEC, 2014).

Estimation of tributary nutrient fluxes

USGS stream gage data was obtained for the Missisquoi River at Swanton, VT, station number 04294000. TN and TP concentration data for the Missisquoi River from 2000 through 2013 were obtained from the Lake Champlain Long-Term Monitoring Program through the Vermont Department of Environmental Conservation website (http://www.anr.state.vt.us/dec/waterq/lakes/htm/lp_longterm.htm).

Tributary fluxes throughout the sampling season were estimated for the Missisquoi River using the EGRET R package v.1.2.4 (Hirsch et al., 2010). This package computes regression surfaces of concentration–discharge relationships weighted by season (Hirsch et al., 2010). Fluxes at the gaging station were scaled to reflect the proportion of the watershed captured by the station (0.98) as well as the proportional contribution of the Missisquoi River to total hydrologic inputs to the bay (0.79) (Limnotech, 2012).

Euphotic depth estimation

Euphotic depth was defined as 1% of irradiance immediately below the water surface, and was estimated from weekly PAR profiles by fitting a curve of Beer's Law:

$$I_z = I_0 \cdot e^{-kz}$$

where I_z is irradiance at depth z, I_0 is surface irradiance, k is the light extinction coefficient, and z is depth. In order to interpolate between weekly measurements, stepwise multiple regression (forward and backward) was used to find the best model for the estimation of euphotic depth based on sonde variables.

Statistics

All statistical analyses were carried out using R statistical software (R Core Team, 2013). Smoothing of PC and Chl-*a* data for visualization was carried out using a smoothing spline with the function *smooth.spline*. Autocorrelation analyses were carried out using the *acf* function, correlations were carried out using the function *cor.test* with Pearson's product–moment correlation ($\alpha < 0.05$), linear and multiple least-squares regressions were carried out using the function *lm* ($\alpha < 0.05$), and model selection was carried out using AIC with the functions *step* and *lm*. Curve fitting was carried out using the function *optim*.

Results and discussion

2012 in historical context

Comprehensive analysis of the historical water quality dataset suggests that in 2012, Missisquoi Bay experienced the strongest bloom within recent years (Fig. 2). To illustrate this point, Fig. 2 shows several metrics of bloom severity from long-term monitoring data from a site close to the sampling location for the current study (Station 51; VT DEC and NY DEC, 2014). Total phosphorus in 2012 was consistently higher throughout the growing season than in any of the previous years. Chl-*a* reached its highest observed concentration in August of 2012, although concentrations during July were somewhat lower than the previous years. pH, an integrated signal of total primary production, was also consistently higher in August of 2012 than in any other year on record. In contrast to these other indicators, total nitrogen was relatively low from June–July, though it increased in August to approach its highest values for the year 2012. Collectively, our analysis of multiple parameters within historical water quality data set from Missisquoi Bay clearly demonstrates that the bloom of 2012 was particularly severe relative to other years.

While recent research in western Lake Erie has found strong correlations between the magnitude of spring discharge and the severity of summer blooms (Stumpf et al., 2012), Missisquoi Bay seems to show a contrasting response. The strong bloom in 2012 occurred during the driest year in the period of record. From May onwards, cumulative discharge from the Missisquoi River was lower than that of any previous calendar year (Fig. 2E). Total phosphorus loading from the Missisquoi River, which is well correlated with discharge (Smeltzer and Simoneau, 2008) was also lower in 2012 than in other years (Fig. 2F). Snowpack in the Missisquoi watershed was also at a historically low level during the winter (http://www.jaypeakresort.com/skiing-riding/the-mountain/snowfall-charts/), suggesting that spring snowmelt and associated P and N loading was also historically low. In contrast, the year 2011 experienced the highest spring TP loading on record due to extensive spring floods (Fig. 2F), but experienced only a modest cyanobacteria bloom (Watzin et al., 2012), and water column concentrations of TP, TN, and Chl-*a* were all unremarkable (Fig. 2). Similarly, the year 2007 which had the highest cumulative spring discharge for the years on record, was also the only year in the past decade in which cyanobacteria did not dominate the phytoplankton community in Missisquoi Bay (Watzin et al., 2008). Assuming maximum water column concentrations of 100 μg P L^{-1} during a strong bloom year (Fig. 2A), uniform concentrations throughout the bay, and bay volume of 0.22 km^3 (Levine et al., 2012), the total mass of P in the water column required to sustain a bloom was calculated to be approximately 22,000 kg (horizontal blue

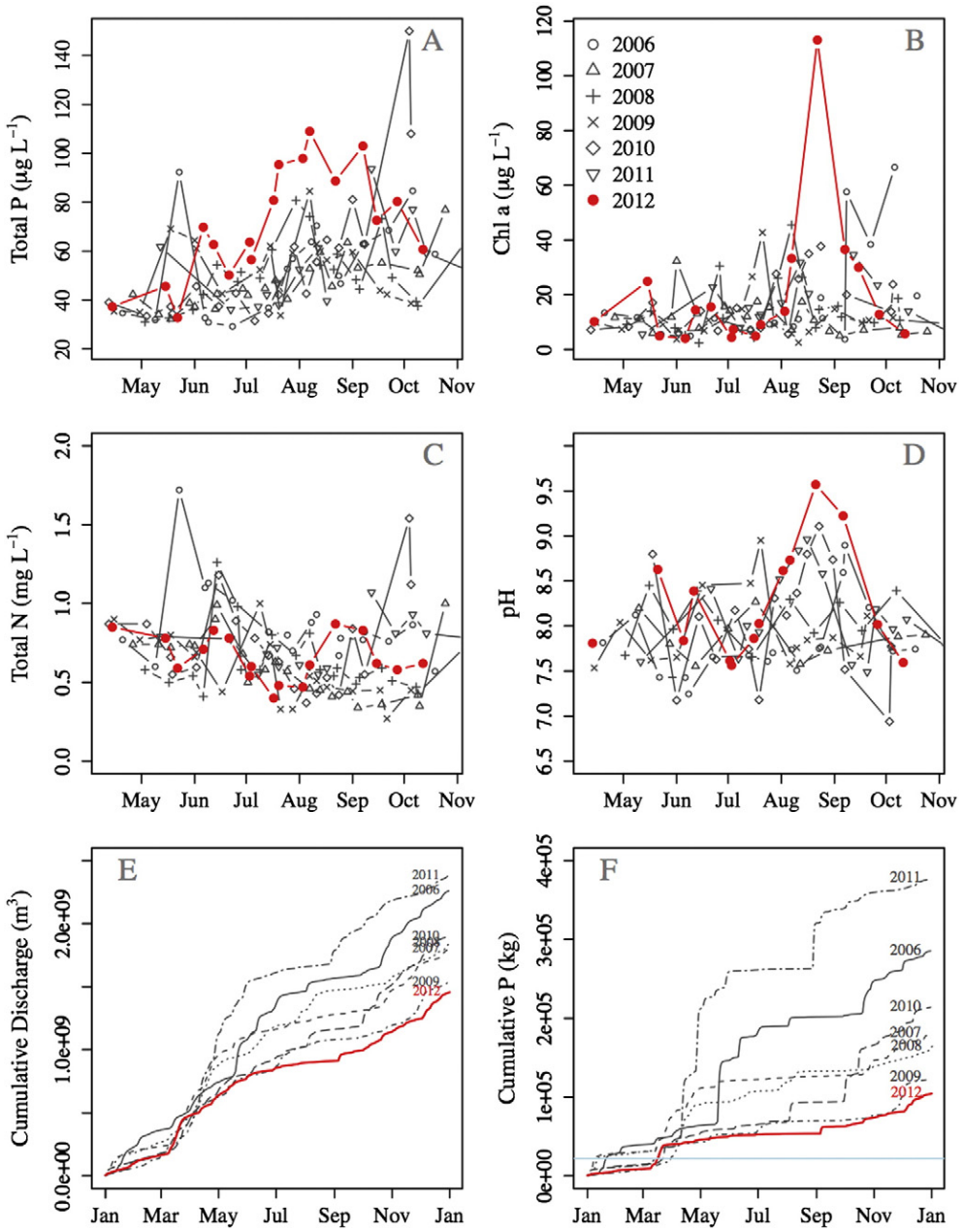

Fig. 2. Comparison of bloom metrics and external loads from long-term monitoring data in Missisquoi Bay (A–D) and the Missisquoi River (E–F), 2006–2012. A: total phosphorus (µg L−1). B: Chlorophyll-*a* (µg L−1). C: total nitrogen (mg L^{-1}). D: pH. 2012 is shown with the red filled circles. E: Cumulative discharge from the Missisquoi River (m^3). F: cumulative TP loading (kg). Blue horizontal line on panel F represents a rough estimate of total water column TP needed to sustain peak bloom conditions (see text).

line on Fig. 2, panel F). This is well below previous records of total spring loading from the Missisquoi River alone, although this does not account for removal pathways. However, in 2012, the highest recorded summer TP in the bay occurred in a year with the lowest spring TP load. This suggests that variation in the internal loading of phosphorus within the bay has had a larger influence on the interannual variability of TP concentrations and bloom dynamics than previously thought.

2012 bloom progression

While useful to provide some historical context of bloom severity and for identification of a primarily internally-driven biogeochemical system in 2012, the composition and temporal resolution of the DEC monitoring dataset limits its utility for describing the mechanisms responsible for bloom dynamics. It was serendipitous, then, that the historical bloom of 2012 also coincided with the deployment of our comprehensive high-frequency, vertically resolved monitoring effort. Indeed, the fact that 2012 was remarkable both for the strength of the summer cyanobacteria bloom and for the lack of external inputs makes it an ideal year for studying the internal drivers of bloom progression in Missisquoi Bay, and the framework and components of our comprehensive monitoring effort provided a powerful tool to study these internal dynamics.

To establish context for the 2012 bloom dynamics, a combined plot of Chl-*a* and PC fluorescence data provides an illustration of the progression throughout the deployment of our monitoring initiative (Fig. 3).

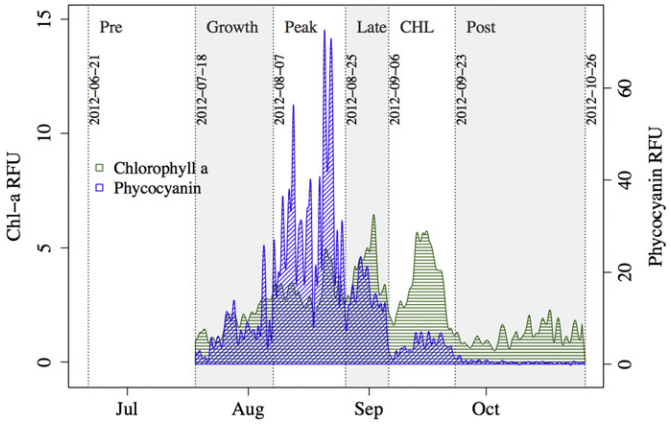

Fig. 3. Spline-smoothed concentrations of chlorophyll-*a* and phycocyanin fluorescence showing the phases of the 2012 bloom. Area with diagonal hatching represents phycocyanin, area with horizontal hatching represents chlorophyll-*a*. Units are ratio fluorescence units, and are not directly comparable between chlorophyll-*a* and phycocyanin. Letters denote bloom phases: Pre = 'pre-bloom', Growth = 'growth phase', Peak = 'peak bloom', Late = 'late bloom', CHL = 'chlorophyll-*a* bloom', Post = 'post-bloom'. These intervals are also used in subsequent plots.

Sensor data show PC rising from near background levels at the middle of July, and reaching sustained levels of ~30 RFU during the middle of August. PC fell during the last week of August and first week of September, but remained fairly high until a storm on 5 September. Following that storm, PC remained low. Chl-*a* largely paralleled PC for most of July and the first half of August, but they became decoupled in late August and early September, with Chl-*a* continuing to increase until the 5 September storm. Following the storm, Chl-*a* rebounded to its highest levels of the season, suggesting increased dominance by eukaryotic algae. The clear trajectory of the bloom as revealed by Chl-*a* and PC fluorescence data allowed us to separate the season into distinct stages of development for discussion and analysis purposes (Fig. 3; Table 1). Six stages are herein discussed: pre-bloom, growth phase, peak bloom, late bloom, chlorophyll bloom, and post-bloom. Of these, the first four occurred with minimal external inputs of nutrients with the exception of the 5 September storm at the end of the late bloom stage, so nutrient dynamics during these stages are considered to be driven by internal processes, which are occurring in conjunction with meteorological forcing (e.g., temperature, light, wind). All of the bloom stages will be discussed with respect to physical drivers, phytoplankton dynamics, nutrient dynamics, and potential limiting resources.

Pre-bloom (21 June through 17 July)

The pre-bloom stage of development coincided with the deployment of our equipment, but logistical challenges associated with sensor deployment precluded automated data collection during this period. As such, we primarily rely on meteorological data from a nearby station and discrete weekly grab sampling to describe the dynamics associated with this phase. The pre-bloom was characterized by low and declining discharge from the Missisquoi River, warm air temperatures, and long days. Water temperature data were not available for this period, but trends from other years indicate that water temperatures were warm and rising through this period. Met data from a nearby monitoring station on the lake indicates that air temperatures were warmer in the pre-bloom period than in the subsequent bloom stages (mean air temperature 22.9 °C during the pre-bloom, compared to 22.7 °C during the growth phase, 22.1 °C during the peak bloom, 21.6 °C during the late bloom, and 18.0 °C during the Chl-*a* bloom) and wind speeds were lower (mean wind speed 3.6 m s^{-1} during the pre-bloom, compared to 4.8 m s^{-1} during the growth phase, 3.5 m s^{-1} during the peak bloom, 5.5 m s^{-1} during the late bloom, and 6.1 m s^{-1} during the Chl-*a* bloom; http://www.uvm.edu/vmc/project/colchester-reef-meteorological-monitoring-38-m). While met data from this station are not directly comparable to data at our monitoring site (Table 1) due to higher average wind speeds and lower air temperature at the main lake station, relative trends between bloom stages are similar. Mean daily solar radiation was also highest during this pre-bloom period (238 W m^{-2}, compared to 211 W m^{-2} during the growth phase, 173 W m^{-2} during the peak bloom, 177 W m^{-2} during the late bloom, and 156 W m^{-2} during the Chl-*a* bloom). Taken together, the temperature, wind speed and solar radiation data allow us to infer that the internal physical drivers that would facilitate nutrient release from the sediment water interface (transient thermal stratification) and increasing phytoplankton productivity (high light and warm water temperatures) were progressively developing during this phase. Indeed, SRP increased over the course of the pre-bloom, while DIN declined (Fig. 5). Higher concentrations of SRP in the bottom water and lower concentrations at the surface were consistent with internal sediment phosphorus loading. The decreases in DIN are likely the result of both uptake by diatoms and denitrification, which has been shown to be highest in Missisquoi Bay in the late spring (McCarthy, 2011). Rising SRP and falling DIN resulted in falling ratios of both DIN:SRP and TN:TP (Figs. 5 and 6).

The phytoplankton community during this period was initially dominated by the diatom *Aulacoseira ambigua*, which declined over the course of this period coincident with increasing populations of *M. aeruginosa* and *D. circinalis* (Fig. 7, ESM Fig. S2), with smaller

Table 1
Phases of the 2012 Bloom Season. Meteorological and water quality data show mean (st. dev.) of the data for each variable for the interval described. River loads are presented as total aggregate load for the bloom stage. All limnological variables are depth-averaged unless otherwise noted. ND indicates no data.

	Pre-bloom	Growth phase	Peak bloom	Late bloom	Chl-*a* bloom	Post-bloom
Dates	29 June–17 July	18 July–6 Aug.	7 Aug.–24 Aug.	25 Aug.–5 Sep.	6 Sep.–22 Sep.	23 Sep.–26 Oct.
Water temp. °C (surface)	ND	25.93 (1.07)	24.98 (1.09)	23.10 (1.42)	19.41 (1.39)	13. 06 (2.34)
Wind speed (m/s)	ND	3.93 (2.18)	3.00 (1.43)	4.15 (2.06)	4.63 (2.37)	4.04 (2.36)
Phycocyanin (RFU)	ND	6.41 (4.87)	25.80 (14.8)	14.39 (4.83)	3.64 (1.92)	0.45 (0.49)
Chl-*a* (RFU)	ND	1.75 (0.80)	3.14 (0.92)	3.99 (2.12)	3.41 (1.59)	1.13 (0.47)
Phycocyanin:Chl-*a*	ND	3.96 (2.90)	8.20 (3.69)	3.88 (1.47)	1.19 (0.83)	0.47 (0.93)
DO mg/L (surface)	ND	10.29 (1.80)	12.14 (2.38)	10.14 (2.50)	9.43 (1.23)	10.01 (0.70)
pH (surface)	ND	9.09 (0.43)	9.76 (0.28)	9.37 (0.48)	8.28 (0.70)	7.67 (0.15)
Euphotic depth (m)	ND	3.76 (0.36)	2.7 (0.57)	2.56 (0.43)	2.98 (0.52)	4.18 (0.21)
TN mg/L	0.41 (0.08)	0.64 (0.28)	1.40 (0.55)	1.39 (0.39)	0.88 (0.17)	0.64 (0.13)
TP mg/L	0.039 (0.0093)	0.078 (0.029)	0.127 (0.044)	0.137 (0.038)	0.087 (0.019)	0.046 (0.017)
TN:TP	25.1 (7.6)	18.2 (4.3)	25.1 (6.8)	23.4 (4.6)	22.5 (2.3)	32.8 (9.0)
River TP load (kg)	970.6	586.2	206.0	7609.6	4142.4	13061.0
River TN load (kg)	23386.7	17874.6	5660.4	32787.1	40086.5	120419.1

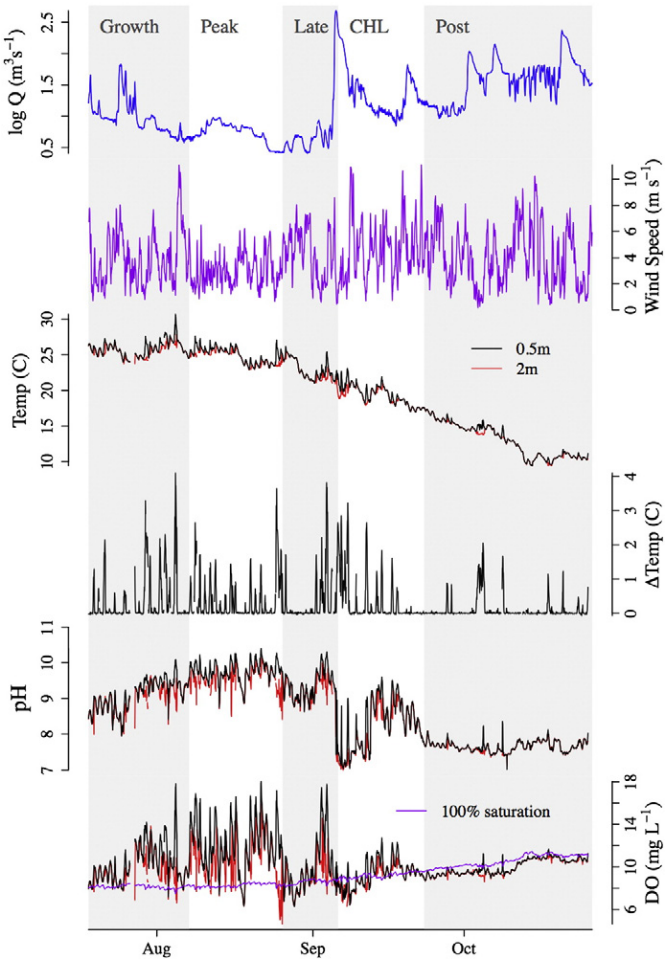

Fig. 4. $\log_{10}$ Missisquoi River Discharge ($m^3\ s^{-1}$), 3 hour running average of wind speed ($m\ s^{-1}$), water temperature at 0.5 m and 2 m (°C), temperature difference between 0.5 m and 2 m (°C), pH at surface and 2 m, and DO ($mg\ L^{-1}$) at 0.5 m and 2 m (with 100% saturation shown in dotted line). Shaded regions represent phases of the bloom (see Fig. 3).

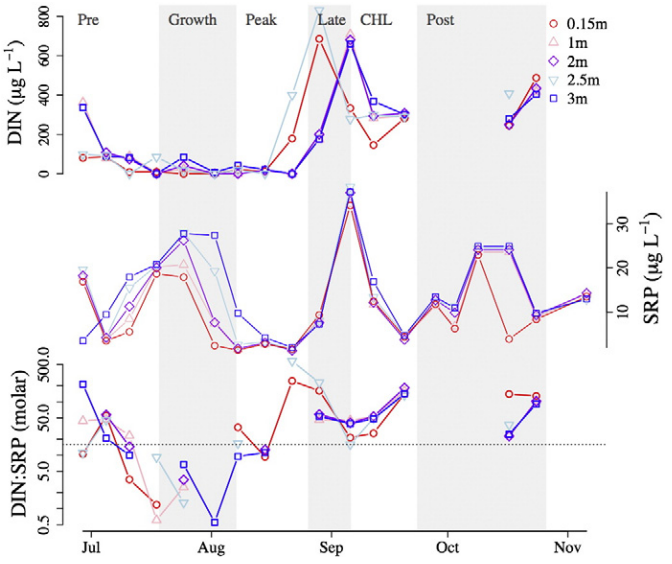

Fig. 5. Dissolved inorganic nitrogen ($\mu g\ L^{-1}$), SRP ($\mu g\ L^{-1}$), and DIN:SRP measured at different depths. Several values of DIN:SRP with DIN below detection limits are omitted due to the logarithmic scale. Dotted line represents the Redfield N:P ratio (16:1). Shaded regions represent phases of the bloom (see Fig. 3).

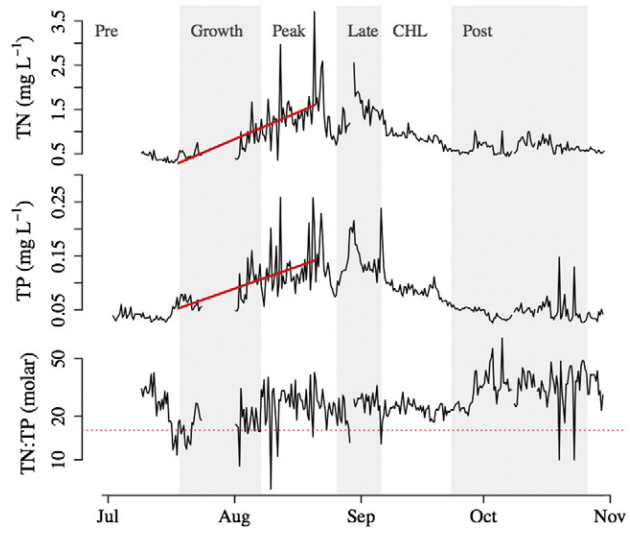

Fig. 6. Total N $mg\ L^{-1}$ (top), TP $mg\ L^{-1}$ (middle) and TN:TP molar ratio (bottom) at an 8-hour timescale, all presented as means of samples from 0.5 m to 2 m depth. Solid lines represent regressions estimating rate of increase of water column TN and TP concentrations during bloom development. Dotted line indicates the Redfield ratio of 16:1. Shaded regions represent phases of the bloom (see Fig. 3).

populations of the morphospecies *M. wesenbergii*, *D. flos-aquae* and *D. crassa*. Populations of smaller phytoplankton may not counted by FlowCAM may have contributed to phytoplankton biovolume during this stage as well. While it is difficult to infer resources limiting production unequivocally at the start of the pre-bloom due to a lack of comprehensive data, as time progressed and internal loading increased water column SRP concentrations while DIN decreased, the system trended towards N limitation. By the end of the pre-bloom, conditions were well primed for the growth of cyanobacterial populations.

Growth phase (18 July through 6 August)

The growth phase consisted of continued warm air and water temperatures and frequent thermal stratification, which was now measured

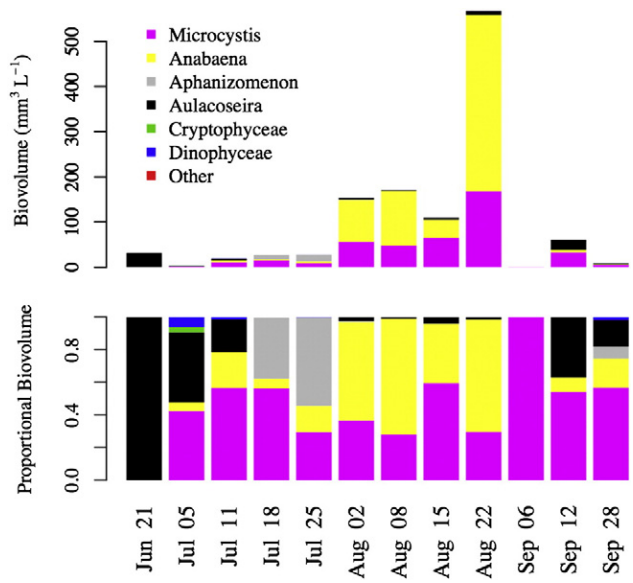

Fig. 7. Biovolume ($mm^3\ L-^1$) and proportional biovolume of large (>25 µm) phytoplankton in Missisquoi Bay from surface samples during the 2012 bloom season.

directly from the automated sensor system (location — Fig. 1, e.g. Fig. 3 and subsequent plots). Water temperatures approached the growth optima for *Microcystis* and *Dolichospermum* during this period (25–30 °C; Paerl et al., 2011). Indeed, populations of cyanobacteria rose throughout the growth phase, while proportions of eukaryotic phytoplankton declined (Figs. 3, 7, ESM Fig. S2). *A. flos-aquae* and *M. aeruginosa* dominated during this phase, with populations of *D. circinalis* increasing during the first week of August. River discharge was low and wind speeds were light and variable throughout this period (Fig. 4). Intermittent calm periods coupled with strong solar radiation contributed to frequent thermal stratification. Factors influencing lake hydrodynamics (river discharge, thermal dynamics, wind speed, solar radiation) all suggest that the system was physically conducive to the continued release of sediment-bound nutrients (Burger et al., 2007, 2008)

The onset of the growth phase coincided with the depletion of available nitrogen and the onset of N-limiting conditions. This is indicated by DIN concentrations, which were very low, by DIN:SRP ratios well below the Redfield ratio, and by TN:TP ratios which were the lowest of the season, and well below 20 which has been cited as a value below which N limitation becomes dominant (Guilford and Hecky, 2000). Further support comes from the emergence of nitrogen-fixing cyanobacteria during this period. The emergence of N-limiting conditions at the onset of bloom development supports the theory that low available N favors the dominance of cyanobacteria with low nitrogen requirements, and particularly N-fixing cyanobacteria (Blomqvist et al., 1994; Herrero et al., 2001).

Despite the scarcity of DIN, TN increased throughout the growth phase. This indicates that there was an additional source of N fueling bloom development. Comparison of loading data and water column concentrations during the growth period makes it clear that the rise in TN cannot be explained by river inputs alone. River TN loads during the growth period (18 July through 20 August, the peak of PC fluorescence) could account for a maximum increase of 3.045 μg L^{-1} d^{-1}, while the average linear rate of increase observed over this period was 35.25 μg L^{-1} d^{-1}. Other possible sources could have been N release from lake sediments or N fixation by cyanobacteria. Previous research in Missisquoi Bay has found the rate of sediment N release to be of a similar order of magnitude to the observed increases in water column TN (McCarthy, 2011), and have found low rates of N-fixation even with large populations of N-fixing cyanobacteria (McCarthy et al., 2013). Heterocyst counts in Nostocales species are generally low in Missisquoi Bay (Angela Shambaugh, Vermont Agency of Natural Resources, personal communication) but the prevalence of *Aphanizomenon* and *Dolichospermum* during the 2012 bloom suggests that N-fixation may have played at least some role in the observed increase of N, although research in other productive systems suggests that this fixation was likely unable to balance N deficiency (Grantz et al., 2014).

The occurrence of N-limiting conditions during the growth phase was in part due to high levels of internal P loading. Total P continued to increase throughout the growth phase, before reaching maximum values in the middle of the peak bloom period (Fig. 6). As with TN, the increase in TP observed during the growth phase and the early part of the peak bloom cannot be explained by river inputs during this period. The linear rate of increase in TP from the onset of the growth phase on 18 July through the highest observed algal concentrations on 20 August (calculated as the mean of TP at 0.5 m and 2 m) was 2.66 μg L^{-1} d^{-1} (Fig. 6, regression line shown in red). During this same period, the maximum potential increase that could be accounted for by river TP flux was 0.102 μg L^{-1} d^{-1}, assuming a bay volume of 0.22 km^3 (Levine et al., 2012). This suggests that while spring loads may be sufficient to explain maximum summer TP concentrations (Fig. 2F), the low TP concentrations during the pre-bloom coupled with the low external flux during the growing season make clear that before river P is made available to phytoplankton it must first be deposited in the sediments. Therefore, the water column P availability during the bloom period is mediated by conditions driving the re-mobilization of sediment P.

The strongest evidence of sediment P mobilization can be seen in the water column SRP concentrations, which remained high during most of the growth phase. High SRP concentrations in the bottom waters and relatively low concentrations in surface waters were consistent with the development of vertical gradients, which would result from the upward diffusion of P from sediments (Fig. 5). The mobilization of sediment P has generally been attributed to the depletion of oxygen at the sediment–water interface (Søndergaard et al., 1999). Dissolved oxygen in Missisquoi Bay generally increased throughout the growth phase of the bloom, reflecting increased primary production in the water column (Fig. 4), and surface concentrations often approached 200% saturation during the day.

Despite the increase in primary production, DO showed transient depth gradients, with oxygen concentrations at 2 m often decreasing during the course of daytime photosynthesis. This stratification of DO was dependent on the development of thermal stratification. The difference in DO between the surface and 2 m ($\Delta DO_{surf-2m}$) for all bloom stages excluding the post-bloom was highly correlated with $\Delta T_{surf-2m}$ during the same period ($R^2 = 0.569$, $p < 0.0001$, n = 1542) (Fig. 8). The slope of the relationship between $\Delta DO_{surf-2m}$ and $\Delta T_{surf-2m}$ was higher during bloom stages with high phytoplankton biomass, indicating that increased water column respiration and decreased light available for photosynthesis allowed increasingly rapid oxygen depletion in the lower water column as the bloom developed (Fig. 8). Dissolved oxygen concentrations at 2 m were often only slightly below 100% saturation on days when the oxygen profile showed stratification; however, manual vertical profiles of dissolved oxygen from 2013 which provide better measurements of O_2 in the bottom water show strong oxygen gradients in the bottom 1 m of the water on calm days (ESM Fig. S3). Even these profiles likely underestimate true oxygen concentrations at the sediment–water interface; previous research has found sharp oxygen gradients on the millimeter scale near the sediment–water interface (Smith et al., 2011), particularly under calm conditions. As a result, we interpret periods of stratification between the surface and 2 m as a proxy for conditions facilitating the development of hypoxia at the sediment–water interface.

The relationship between $\Delta DO_{surf-2m}$ and $\Delta T_{surf-2m}$ supports the conclusion that the internal flux of phosphorus was driven by transient thermal stratification resulting in bottom water oxygen depletion and reductive dissolution of Fe and Mn oxyhydroxides. This is further supported by the geochemical data. Dissolved Fe and Mn in water taken at 3 m were tested for correlations with total dissolved P at the same depth. No significant correlations were found for Fe, but dissolved Mn was significantly positively correlated with total dissolved P as measured by ICP-MS ($R^2 = 0.42$, $p = 0.030$; n = 11). Manganese is more easily reduced than Fe, which may make it a more sensitive indicator of the occurrence of transient stratification than dissolved Fe in Missisquoi Bay (Pearce et al., 2013). The presence of dissolved Mn in the lower water column is another indicator that reducing conditions were present in the bottom water even when DO concentrations at 2 m depth were close to saturation. Taken together, the DO, metals, and SRP data confirm the hypothesis that internal loading is driven by transient thermal stratification and resulting bottom water reducing conditions. Furthermore, the effects of transient stratification are magnified during periods of high biomass, which may constitute a positive feedback for maintaining bloom conditions. The frequent thermal stratification and the rise in water column TP observed during the growth phase suggest that these processes were particularly important in fueling the rapid growth of cyanobacteria populations in 2012.

Peak bloom (8 August through 24 August)

During the peak bloom, river discharge was at a minimum and average wind speeds were consistently low, rarely rising over 4.5 m s^{-1} (Fig. 4; Table 1). These conditions resulted in frequent periods of thermal stratification during daylight hours and provided a thermal

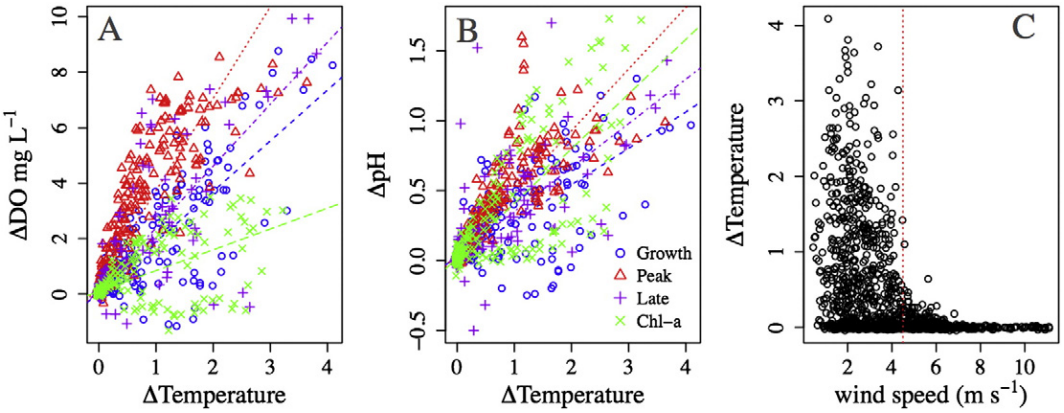

Fig. 8. Panel A: Thermal stratification between 0.5 and 2 m (°C) vs. stratification in DO (mg L^{-1}). Point types represent samples from different stages of the bloom: circle = growth phase, triangle = peak bloom, cross = late bloom, and x = chl-*a* bloom. Lines represent linear regressions for each bloom stage. Panel B: Thermal stratification (°C) vs. stratification in pH. Panel C: Thermal stratification (°C) vs. 3-hour running average of wind speed (m s^{-1}). Vertical line is at 4.5 m s^{-1}.

structure, which was conducive to the continued release of sediment bound P. During the peak bloom, phytoplankton biovolume reached the maximum of the season. The phytoplankton community was largely comprised of *Dolichospermum* and *Microcystis* spp. (Fig. 7), suggesting that ecosystem demands for both N and P would also be extremely high during this phase.

A high biological demand for nutrients would explain the rapidly declining SRP concentrations that occurred during the peak bloom. The drop in SRP concentrations below detection limits coincided with the peak of algal biovolume. TN and TP were high and were correlated with PC, suggesting that most of the water column nutrients were associated with cyanobacterial biovolume. TP continued to rise for most of the peak bloom, which must be fueled by sediment P release (as indicated by the lack of external inputs) but fell at the end of the period paralleling the decline in cyanobacteria populations.

In addition to the role of reductive dissolution, elevated pH due to high photosynthetic activity may have also played a role in promoting release of sediment P during the peak bloom. Previous research has found that pH above 9 can accelerate sediment P flux (Boers, 1991; Jensen and Andersen, 1992; Jin et al., 2006; Seitzinger, 1991). In Missisquoi Bay, surface pH remained between 9 and 10.5 throughout this period (Fig. 4). The effects of this high pH on sediment nutrient release may be mitigated by the steep pH gradients that occur near the sediment water interface during calm conditions (Smith et al., 2011), but high pH may help to sustain P flux during mixed conditions when boundary layers are less pronounced.

Total N tracked PC concentrations closely, rising for most of the peak bloom but declining towards the end. As described for the TP trends, this indicates that most of the nutrients in the system were incorporated into algal biomass during the peak bloom period. The decrease in cyanobacteria biovolume at the end of the peak bloom period coincided with marked increases in DIN, consistent with the remineralization of algal N.

The TN:TP ratio rose throughout the growth phase and peak bloom. TN:TP (calculated using an average of concentrations at 0.5 m and 2 m) was positively correlated with cyanobacterial abundance during the growth period, from the start of automated data collection through the period of highest PC concentrations on 25 August ($R^2 = 0.20$, $p < 0.0001$, n = 90). This rise in TN:TP sheds light on the debate about the relationship of TN:TP with cyanobacterial dominance (Smith, 1983). In this dataset, low TN:TP coincided with the onset of cyanobacterial growth, but during the bloom itself, TN:TP is positively correlated with PC. The rise in TN:TP during bloom development may be partly attributable to light limitation, which has been shown to affect algal N:P through the increasing allocation of cellular resources to nitrogen-rich photosynthetic machinery (Sterner et al., 1997; Sterner and Elser, 2002), rather than to the easing of N-limitation. It may also reflect the fact that heterocystous cyanobacteria such as *Dolichospermum* tend to have higher optimal internal N:P content than other colonial cyanobacteria (Klausmeier et al., 2004), and that these populations represented an increasing proportion of the phytoplankton community during bloom development.

The peak bloom was characterized by multiple scarce resources including DIN, SRP, and light. Light scarcity resulted from high cell concentrations and was reflected in shallow euphotic depths (Table 1). The generally low wind speeds during the peak bloom likely favored dominance by positively-buoyant cyanobacteria by allowing them to access limited light resources despite these shallow euphotic depths (Huisman et al., 2004; Reynolds et al., 1987). Low DIN serves as an indication of continued N scarcity, particularly under light limited conditions when N fixation may be suppressed (de Tezanos Pinto and Litchman, 2010), while the depletion of SRP at the peak of cyanobacteria biovolume suggests that cyanobacteria were approaching carrying capacity relative to benthic P supply, and that P limitation played a role in the subsequent decline of cyanobacteria populations.

Late bloom (25 August through 5 September)

During the late bloom, river discharge remained low, indicating that nutrient dynamics were still being driven primarily by internal dynamics. Cyanobacteria biovolume was still high but decreasing during the late bloom, and there were increased proportions of eukaryotic phytoplankton (evidenced by decreased PC:Chl-*a*; Table 1, Fig. 7). Water temperature declined gradually throughout this period, and water temperatures were rarely stratified due to greater winds. Fig. 8C shows that above a threshold of 4.5 m s^{-1}, thermal stratification is inhibited by wind mixing. While wind speeds during the peak bloom generally remained below this threshold (Fig. 4), wind speeds were above this threshold for most of the late-bloom period. Since thermal and related DO stratification of the water column was clearly limited due to wind mixing, conditions during the late bloom were not conducive to redox-driven benthic nutrient release. However, both SRP and DIN were present in moderate and increasing quantities during the late bloom, suggesting that another internal source and or mechanism was responsible for their availability (Fig. 5). These moderate dissolved nutrient concentrations were likely due to the recycling of cell-derived P and N due to remineralization of peak bloom algal nutrients as the peak bloom died off. It is likely that the biogeochemical feedbacks in this system fundamentally changed in response to a more mixed and turbulent water column. Additionally, desorption of P at the sediment–water interface could provide a source of SRP during these mixed conditions if pH at the SWI was raised above ~9 (the zero point of charge of Mn/Fe (oxy) hydroxides), which may be possible if bottom turbulence was sufficient to erode highly buffered boundary layers (L. Smith et al., 2011;

Thomas and Schallenberg, 2008). The moderate available concentrations of DIN and SRP also suggest that another factor was limiting phytoplankton populations during the late bloom.

Indeed, our sensor data reveals that the euphotic depth was at its shallowest of the season during the late bloom (Table 1). The combination of shallow euphotic depth with frequent mixed conditions may have overcome the potential for buoyancy regulation by cyanobacteria, which may have contributed to net population growth during the peak bloom despite shallow euphotic depths by bringing the cells closer to the surface and available light to stimulate growth (Ganf and Oliver, 1982; Reynolds et al., 1987). The ample concentrations of available N and P, in combination with the evidence of light scarcity and the prolonged period of wind mixing, suggest that light was the primary limiting resource during this period. This conclusion is further supported by the occurrence of DO concentrations which were below saturation at all depths during the first half of this period (Fig. 4), suggesting that primary production was suppressed despite large populations of phytoplankton and that respiratory losses and decomposition were sufficient to overcome reaeration. DO rose at the end of this period as wind speeds subsided and primary production increased (Fig. 4), and there was a short-lived increase in PC during these calm conditions (Fig. 3), further supporting the conclusion that light limitation induced by wind mixing was responsible for the declines during the early part of the late-bloom period. These highly dynamic shifts in production and wind mixing were only observable as a result of our high-frequency, vertically resolved sensor array, highlighting the power of our approach in identifying and quantifying dynamics that would likely be missed or mischaracterized using a conventional monitoring approach.

Chl-a bloom (6 September through 22 September)

The first major storm of the summer occurred on 4 September through 5 September (Figs. 3, 8), and had dramatic impacts on the progression of the bloom, marking the end of the late bloom and the beginning of the Chl-*a* bloom. The Chl-*a* bloom was given that name because it was characterized by high Chl-*a* fluorescence but low PC fluorescence, indicating a shift in relative abundance from cyanobacteria to eukaryotic phytoplankton (predominantly *Aulacoseira*, Fig. 7, ESM Fig. S2), although cyanobacteria remained the largest component of total phytoplankton biovolume (and may have been underrepresented in the FlowCAM data if colonies had broken into small fragments during senescence). Smaller eukaryotes not measured by the FlowCAM may also have increased during this period. The increases in *Aulacoseira* may be partly attributable to the resuspension of sedimented cells with increased turbulence during the storm. Following the storm event, the physical drivers of the system changed relative to the previous bloom stages. The Chl-*a* bloom stage was physically characterized by relatively high winds and river discharge coupled with progressively declining air and water temperature (Fig. 4). Thermal stratification was infrequent during this period due to cooling and hydrodynamic disturbance from wind and river discharge, indicating another change in the physical drivers of nutrient and ecosystem dynamics.

PC and Chl-*a* fluorescence declined sharply and almost instantaneously in response to the storm event, suggesting that flushing and dilution displaced the extant phytoplankton populations within the bay. The chemical environment was also strongly impacted by the storm event. Remarkably, in the space of 2 days pH dropped by close to 3 units and DO dropped and remained relatively low throughout the rest of the monitoring period (Fig. 4), likely driven by dramatic decreases in water column photosynthetic activity and coupled with the influx of more acidic river water. After the storm moved through, DO and pH were rarely stratified due to lower primary production and reduced thermal stratification. Total N and TP dropped immediately following the storm corresponding to the drop in phytoplankton biovolume and related cell-bound nutrients; these drops were likely due to sedimentation of senescing cells as well as flushing effects. Following the storm, TN and TP continued to decline throughout the Chl-*a* bloom period. In contrast to the drop in TN and TP, both SRP and DIN were high immediately following the storm, which provided a dramatic influx of soluble available nutrients, likely associated with nonpoint source pollution from the Missisquoi Bay's highly agricultural watershed (Smeltzer and Simoneau, 2008). Subsequently, SRP declined over the course of the period, while DIN remained high, resulting in DIN:SRP ratios well above 16.

The storm that occurred at the beginning of the Chl-*a* bloom period appeared to shift the competitive balance between cyanobacteria and eukaryotic phytoplankton by delivering available nutrients and increasing water clarity and light availability. While this process was likely underway already as a result of decreasing water temperatures and decreasing day length (which may trigger akinete formation in Nostocales), the storm event appeared to accelerate this transition and prevent the occurrence of late-season cyanobacteria blooms, which sometimes occur in Missisquoi Bay. Observing the impact of this storm would have been difficult without the combination of a high-frequency monitoring array and an adjacent USGS gage site; using only bi-weekly monitoring data that did not resolve the immediacy of the storm's impacts, it would have been difficult to attribute changes in the phytoplankton community and chemical environment to the storm event rather than gradual successional processes.

Post-bloom (23 September through 26 October)

The post-bloom period was characterized by low water temperatures, high winds, and high river discharge. During this time frame, water temperatures dropped from 17 °C to 10 °C, making them sufficiently low to depress growth rates for most bloom-forming phytoplankton in Missisquoi Bay (Butterwick et al., 2005). PC and Chl-*a* were low during this period, confirming that phytoplankton biomass was low. The ratio of TN:TP was at its highest during the post-bloom with a mean value of 32 (Table 1), suggesting that the system was stoichiometrically P-limited, but the high levels of DIN and SRP during this period demonstrate the neither nutrient was the limiting resource of the bay's phytoplankton population. The low and progressively decreasing water temperature and solar radiation were likely the key factors limiting growth rates during this period.

Conclusions

The strongest bloom in recent years in Missisquoi Bay occurred in 2012 when tributary discharge was near historic lows, making it an ideal year for studying cyanobacteria bloom progression as a function of internal processes in this system. We were well poised to study these internal nutrient dynamics because of a comprehensive, cutting-edge monitoring effort that coincidentally began in early summer 2012, and many details would have been missed or mischaracterized using only data from traditional water quality monitoring efforts. High-frequency data were used to partition the bloom into distinct stages of growth, maintenance, and decline, and allowed us to describe the physical, chemical, and biological processes driving bloom dynamics during these stages. Many of the internal processes that affected the balance of resource limitation were influenced by the effects of wind on water column stability. On a seasonal scale the onset of N limitation was dependent on the release of sediment P, and the benthic oxygen depletion that fueled this release was dependent on calm, stratified periods. As algal biovolume and respiration increased, shorter periods of thermal stratification were sufficient to induce stratification in dissolved oxygen (Fig. 8), which likely resulted in the more rapid development of reducing conditions at the sediment water interface (ESM Fig. S3) constituting a feedback that may have helped to sustain bloom conditions. In addition to its effects on sediment nutrient release, wind mixing also mediated competition for light in this system by

overcoming cyanobacterial buoyancy regulation in the later stages of the bloom.

We demonstrate that, contrary to expectations from recent studies in western Lake Erie (Stumpf et al., 2012), high spring discharge does not appear to be the dominant factor controlling interannual variability in the severity of summertime cyanobacteria blooms in Missisquoi Bay. If anything, the data suggest that Missisquoi Bay may have the opposite relationship to spring discharge, with years of low external loads corresponding to stronger blooms. We hypothesize that this may be a function of the N:P balance. In 2012, the growth period for cyanobacteria was initiated during a period with low N:P. While P loading from the sediments is driven largely by internal processes, TN concentrations in every year are highest in the spring following the snowmelt period, suggesting that external loading may control nitrogen availability more than P availability. As a result, low spring discharge in combination with spring populations of N-consuming phytoplankton may actually promote cyanobacteria blooms in Missisquoi bay by inducing N-limited conditions in which cyanobacteria are more likely to dominate (Smith, 1983). This is consistent with long-term monitoring data, which show very low TN concentrations in 2012 during the pre-bloom period relative to other years, and warrants further study.

While this paper highlights the role of internal cycling, it is critical to note here that the ultimate source of the enrichment of benthic P that drove the bloom was the watershed, and the key factor responsible for eutrophic conditions ultimately remains historical and current loading from the agricultural catchment. The dramatic impact of the 5 September storm provides a further illustration of the importance of watershed processes on the lake system. In the space of several days the storm resulted in a drop in pH of almost 3 units, large increases in the concentrations of available nutrients in the system, and a shift in dominance from cyanobacteria to eukaryotic phytoplankton. Storms may have particularly strong influences late in the summer, when decreasing water temperatures depress cyanobacteria growth rates. Missisquoi Bay may be particularly susceptible to the effects of discharge due to the high ratio of watershed area to lake volume, and studying the effects of similar storms requires high-frequency data capable of capturing the rapidly evolving response of the system to storm events.

This work illustrates the power of synthesizing long-term water quality monitoring data with high-frequency sensor data and intensive sampling programs to allow for more detailed and process-based monitoring studies. Similar efforts to describe these processes across multiple time-scales in this and other lakes may ultimately yield a deeper understanding of lake processes. This study is by nature limited by its lack of spatial resolution; while Missisquoi Bay is largely homogeneous with respect to depth and sediment composition, the deployment of more limited sensor arrays at additional sites would help to quantify the extent of spatial variability in the future. Findings in this study may be applicable to shallow bays of the Great Lakes and elsewhere. While the individual mechanisms described herein may not be novel, the ability to examine many aspects of this system using a unique dataset in a historically strong bloom year with a clear trajectory of growth and decline provides an unusually clear picture of how these mechanisms may interact to drive cyanobacteria bloom progression.

Acknowledgments

Support provided by Vermont EPSCoR with funds from the National Science Foundation Grant EPS-1101317 is greatly acknowledged. Any opinions, findings, and conclusions or recommendations expressed in this material are those of the authors and do not necessarily reflect the views of the National Science Foundation. Thanks to two anonymous reviewers, as well as to Steve Cluett for invaluable assistance in the deployment and design of field equipment, Elissa Schuett for assistance with maintenance of the monitoring equipment, Saul Blocher of Johnson State College for processing nutrient samples, Dr. Wiebke Boeing of New Mexico State University for access to a FlowCAM, Dr. Jason Stockwell of the University of Vermont for comments which greatly improved the quality of this manuscript and Fluid Imaging Technologies for a temporary equipment grant providing a FlowCAM and associated software for further analyses.

Appendix A. Supplementary data

Supplementary data to this article can be found online at http://dx.doi.org/10.1016/j.jglr.2015.06.006.

References

Álvarez, E., Moyano, M., López-Urrutia, Á., Nogueira, E., Scharek, R., 2013. Routine determination of plankton community composition and size structure: a comparison between FlowCAM and light microscopy. J. Plankton Res. 36, 170–184. http://dx.doi.org/10.1093/plank/fbt069.

Anderson, D.M., Cembella, A.D., Hallegraeff, G.M., 2012. Progress in understanding harmful algal blooms: paradigm shifts and new technologies for research, monitoring, and management. Ann. Rev. Mar. Sci. 4, 143–176. http://dx.doi.org/10.1146/annurev-marine-120308-081121.

APHA, 2005. Standard Methods for the Examination of Water and Wastewater, 21st ed American Public Health Association (APHA), the American Water Works Association (AWWA), and the Water Environment Federation (WEF), Washington, D.C. (USA).

Baker, A.L., et al., 2012. Phycokey — an image based key to algae (PS Protista), cyanobacteria, and other aquatic objects. University of New Hampshire Center for Freshwater Biology. http://cfb.unh.edu/phycokey/phycokey.htm (3 Mar 2014).

Blomqvist, P., Pettersson, A., Hyenstrand, P., 1994. Ammonium–nitrogen: a key regulatory factor causing dominance of non-nitrogen-fixing cyanobacteria in aquatic systems. Archiv. Hydrobiol. 132, 141–164.

Boers, P., 1991. The influence of pH on phosphate release from lake sediments. Water Res. 25, 309–311.

Burger, D.F., Hamilton, D.P., Pilditch, C.A., Gibbs, M.M., 2007. Benthic nutrient fluxes in a eutrophic, polymictic lake. Hydrobiologia 584, 13–25. http://dx.doi.org/10.1007/s10750-007-0582-0.

Burger, D.F., Hamilton, D.P., Pilditch, C.A., 2008. Modelling the relative importance of internal and external nutrient loads on water column nutrient concentrations and phytoplankton biomass in a shallow polymictic lake. Ecol. Model. 211, 411–423. http://dx.doi.org/10.1016/j.ecolmodel.2007.09.028.

Burgin, A., Hamilton, S., 2007. Have we overemphasized the role of denitrification in aquatic ecosystems? A review of nitrate removal pathways. Front. Ecol. Environ. 5, 89–96.

Butterwick, C., Heaney, S.I., Talling, J.F., 2005. Diversity in the influence of temperature on the growth rates of freshwater algae, and its ecological relevance. Freshw. Biol. 50, 291–300. http://dx.doi.org/10.1111/j.1365-2427.2004.01317.x.

Carpenter, S.R., Kitchell, J.F., 1987. The temporal scale of variance in limnetic primary production. Am. Nat. 129, 417–433.

Carpenter, S.R., Kitchell, J.F., Hodgson, J.R., 1985. Cascading trophic interactions and lake productivity. Bioscience 35, 634–639.

Chaffin, J.D., Bridgeman, T.B., Bade, D.L., 2013. Nitrogen constrains the growth of late summer cyanobacterial blooms in Lake Erie. AiM 03, 16–26. http://dx.doi.org/10.4236/aim.2013.36A003.

Core Team, R., 2013. R: A Language and Environment for Statistical Computing. R Foundation for Statistical Computing, Vienna, Austria (URL http://www.R-project.org/).

de Tezanos Pinto, P., Litchman, E., 2010. Interactive effects of N:P ratios and light on nitrogen-fixer abundance. Oikos 119, 567–575. http://dx.doi.org/10.1111/j.1600-0706.2009.17924.x.

Dokulil, M., Teubner, K., 2000. Cyanobacterial dominance in lakes. Hydrobiologia 438, 1–12.

Facey, D.E., Marsden, J.E., Mihuc, T.B., Howe, E.A., 2012. J. Great Lakes Res. 38, 1–5. http://dx.doi.org/10.1016/j.jglr.2011.12.001.

Ganf, G.G., Oliver, R.L., 1982. Vertical separation of light and available nutrients as a factor causing replacement of green algae by blue-green algae in the plankton of a stratified lake. J. Ecology 829–844.

Gerten, D., Adrian, R., 2000. Climate-driven changes in spring plankton dynamics and the sensitivity of shallow polymictic lakes to the North Atlantic Oscillation. Limnol. Oceanogr. 45, 1058–1066.

Grantz, E.M., Haggard, B.E., Scott, J.T., 2014. Stoichiometric imbalance in rates of nitrogen and phosphorus retention, storage, and recycling can perpetuate nitrogen deficiency in highly-productive reservoirs. Limnol. Oceanogr. 59, 2203–2216.

Guilford, S.J., Hecky, R.E., 2000. Total nitrogen, total phosphorus, and nutrient limitation in lakes and oceans: is there a common relationship? Limnol. Oceanogr. 45, 1213–1223.

Herrero, A., Muro-Pastor, A.M., Flores, E., 2001. Nitrogen control in cyanobacteria. J. Bacteriol. 183, 411–425. http://dx.doi.org/10.1128/JB.183.2.411-425.2001.

Hirsch, R.M., Moyer, D.L., Archfield, S.A., 2010. Weighted regressions on time, discharge, and season (WRTDS), with an application to Chesapeake Bay river inputs. J. Am. Water Resour. Assoc. 46, 857–880. http://dx.doi.org/10.1111/j.1752-1688.2010.00482.x.

Huisman, J., van Oostveen, P., Weissing, F.J., 1999. Species dynamics in phytoplankton blooms: incomplete mixing and competition for light. Am. Nat. 154, 46–68. http://dx.doi.org/10.1086/303220.

Huisman, J., Sharples, J., Stroom, J.M., Visser, P.M., Kardinaal, W.E.A., Verspagen, J.M.H., Sommeijer, B., 2004. Changes in turbulent mixing shift competition for light between phytoplankton species. Ecology 85, 2960–2970.
Hupfer, M., Lewandowski, J., 2008. Oxygen controls the phosphorus release from lake sediments — a long-lasting paradigm in limnology. Int. Rev. Hydrobiol. 93, 415–432. http://dx.doi.org/10.1002/iroh.200711054.
Jennings, E., Jones, S., Arvola, L., Staehr, P.A., Gaiser, E., Jones, I.D., Weathers, K.C., Weyhenmeyer, G.A., Chiu, C.-Y., De Eyto, E., 2012. Effects of weather-related episodic events in lakes: an analysis based on high-frequency data. Freshw. Biol. 57, 589–601. http://dx.doi.org/10.1111/j.1365-2427.2011.02729.x.
Jensen, H., Andersen, F., 1992. Importance of temperature, nitrate, and pH for phosphate release from aerobic sediments of four shallow, eutrophic lakes. Limnol. Oceanogr. 37, 577–589.
Jeppesen, E., Jensen, J., Søndergaard, M., Lauridsen, T., Pedersen, L., Jensen, L., 1997. Top-down control in freshwater lakes: the role of nutrient state, submerged macrophytes and water depth. Hydrobiologia 342, 151–164.
Jin, X., Wang, S., Pang, Y., Chang Wu, F., 2006. Phosphorus fractions and the effect of pH on the phosphorus release of the sediments from different trophic areas in Taihu Lake. China. Environ. Pollution 139, 288–295. http://dx.doi.org/10.1016/j.envpol.2005.05.010.
Klausmeier, C.A., Litchman, E., Daufresne, T., Levin, S.A., 2004. Optimal nitrogen-to-phosphorus stoichiometry of phytoplankton. Nature 429, 171–174. http://dx.doi.org/10.1038/nature02508.
Kolzau, S., Wiedner, C., Rücker, J., Kohler, J., Köhler, A., Dolman, A.M., 2014. Seasonal patterns of nitrogen and phosphorus limitation in four German lakes and the predictability of limitation status from ambient nutrient concentrations. PLoS ONE 9. http://dx.doi.org/10.1371/journal.pone.0096065.s003 e96065.
Komarek, J., Zapomelova, E., 2007. Planktic morphospecies of the cyanobacteria genus Anabaena = subg. Dolichospermum—1. Part: coiled types. Fottea 7, 1–31.
Levin, S.A., 1992. The problem of pattern and scale in ecology: the Robert H. MacArthur award lecture. Ecology 73, 1943–1967.
Levine, S.N., Lini, A., Ostrofsky, M.L., Bunting, L., Burgess, H., Leavitt, P.R., Reuter, D., Lami, A., Guilizzoni, P., Gilles, E., 2012. The eutrophication of Lake Champlain's northeastern arm: insights from paleolimnological analyses. J. Great Lakes Res. 38, 35–48. http://dx.doi.org/10.1016/j.jglr.2011.07.007.
Limnotech, 2012. Development of a Phosphorus Mass Balance Model for Missisquoi Bay. Lake Champlain Basin Program Technical Report 65, pp. 1–89.
Litke, D.W., 1999. Review of Phosphorus Control Measures in the United States and Their Effects on Water Quality. U.S. Geological Survey NWQAP.
McCarthy, M.J., 2011. Nitrogen Availability and Transformations in Missisquoi Bay, Lake Champlain: Effects on Phytoplankton Community Structure and Cyanobacterial Blooms (Ph.D. Dissertation) Université du Québec a Montréal, pp. 1–203.
McCarthy, M.J., Gardner, W.S., Lehmann, M.F., Bird, D.F., 2013. Implications of water column ammonium uptake and regeneration for the nitrogen budget in temperate, eutrophic Missisquoi Bay, Lake Champlain (Canada/USA). Hydrobiologia 718, 173–188. http://dx.doi.org/10.1007/s10750-013-1614-6.
McGill, B.J., 2010. Matters of scale. Science 328, 575–576. http://dx.doi.org/10.1126/science.1188528.
McQuaid, N., Zamyadi, A., Prévost, M., Bird, D.F., Dorner, S., 2011. Use of in vivo phycocyanin fluorescence to monitor potential microcystin-producing cyanobacterial biovolume in a drinking water source. J. Environ. Monit. 13, 455. http://dx.doi.org/10.1039/c0em00163e.
Michalak, A., Anderson, E., Beletsky, D., Boland, S., Bosch, N.S., Bridgeman, T.B., Chaffin, J.D., Cho, K., Confesor, R., Daloglu, I., DePinto, J.V., Evans, M.A., Fahnesnstiel, G.L., He, L., Ho, J.C., Jenkins, L., Johengen, T.H., Kuo, K.C., LaPorte, E., Liu, X., McWilliams, M.R., Moore, M.R., Posselt, D.J., Richards, R.P., Scavia, D., Steiner, A.L., Verhamme, E., Wright, D.M., Zagorski, M.A., 2013. Record-setting algal bloom in Lake Erie caused by agricultural and meteorological trends consistent with expected future conditions. Proc. Natl. Acad. Sci. 110, 6448–6452. http://dx.doi.org/10.1073/pnas.1216006110.
Muro-Pastor, M.I., Reyes, J.C., Florencio, F.J., 2005. Ammonium assimilation in cyanobacteria. Photosynth. Res. 83, 135–150. http://dx.doi.org/10.1007/s11120-004-2082-7.
Paerl, H.W., Huisman, J., 2009. Climate change: a catalyst for global expansion of harmful cyanobacterial blooms. Environ. Microbiol. Rep. 1, 27–37. http://dx.doi.org/10.1111/j.1758-2229.2008.00004.x.
Paerl, H.W., Hall, N.S., Calandrino, E.S., 2011. Controlling harmful cyanobacterial blooms in a world experiencing anthropogenic and climatic-induced change. Sci. Total Environ. 409, 1739–1745. http://dx.doi.org/10.1016/j.scitotenv.2011.02.001.
Pearce, A.R., Rizzo, D.M., Watzin, M.C., Druschel, G.K., 2013. Unraveling associations between cyanobacteria blooms and in-lake environmental conditions in Missisquoi Bay, Lake Champlain, USA, using a modified self-organizing map. Environ. Sci. Technol. 47, 14267–14274. http://dx.doi.org/10.1021/es403490g.
Pierson, D.C., Samal, N.R., Owens, E.M., Schneiderman, E.M., Zion, M.S., 2013. Changes in the timing of snowmelt and the seasonality of nutrient loading: can models simulate the impacts on freshwater trophic status? Hydrol. Process. 27, 3083–3093. http://dx.doi.org/10.1002/hyp.9894.
Piña-Ochoa, E., Álvarez-Cobelas, M., 2006. Denitrification in aquatic environments: a cross-system analysis. Biogeochemistry 81, 111–130. http://dx.doi.org/10.1007/s10533-006-9033-7.
Prescott, G.W., 1962. Algae of the Western Great Lakes Area With an Illustrated Key to the Genera of Desmids and Freshwater Diatoms. WM.C. Brown Company Publishers.
Prescott, G.W., 1978. How to Know the Freshwater Algae. Pictured Key Nature Series, 3rd edition W.M.C. Brown Company Publishers.
Reitzel, K., Ahlgren, J., Rydin, E., Egemose, S., Turner, B.L., Hupfer, M., 2012. Diagenesis of settling seston: identity and transformations of organic phosphorus. J. Environ. Monit. 14, 1098. http://dx.doi.org/10.1039/c2em10883f.
Reynolds, C.S., Oliver, R.L., Walsby, A.E., 1987. Cyanobacterial dominance: the role of buoyancy regulation in dynamic lake environments. N. Z. J. Mar. Freshw. Res. 21, 379–390. http://dx.doi.org/10.1080/00288330.1987.9516234.
Schindler, D.W., 1977. Evolution of phosphorus limitation in lakes. Science 195, 260–262. http://dx.doi.org/10.1126/science.195.4275.260.
Schindler, D.W., 2012. The dilemma of controlling cultural eutrophication of lakes. Proc. R. Soc. B Biol. Sci. 279, 4322–4333. http://dx.doi.org/10.1098/rspb.2012.1032.
Scott, J.T., McCarthy, M.J., 2010. Nitrogen fixation may not balance the nitrogen pool in lakes over timescales relevant to eutrophication management. Limnol. Oceanogr. 55, 1265–1270. http://dx.doi.org/10.4319/lo.2010.55.3.1265.
Seitzinger, S.P., 1991. The effect of pH on the release of phosphorus from Potomac estuary sediments: implications for blue-green algal blooms. Estuar. Coast. Shelf Sci. 33, 409–418.
Smeltzer, E., Simoneau, M., 2008. Phosphorus Loading to Missisquoi Bay From Sub-Basins in Vermont and Québec, 2002–2005. Lake Champlain Steering Committee. pp. 1–22.
Smeltzer, E., Shambaugh, A.D., Stangel, P., 2012. Environmental change in Lake Champlain revealed by long-term monitoring. J. Great Lakes Res. 38, 6–18. http://dx.doi.org/10.1016/j.jglr.2012.01.002.
Smith, V.H., 1983. Low nitrogen to phosphorus ratios favor dominance by blue-green algae in lake phytoplankton. Science 221, 669–671. http://dx.doi.org/10.1126/science.221.4611.669.
Smith, V.H., Schindler, D.W., 2009. Eutrophication science: where do we go from here? Trends Ecol. Evol. 24, 201–207. http://dx.doi.org/10.1016/j.tree.2008.11.009.
Smith, L., Watzin, M.C., Druschel, G., 2011. Relating sediment phosphorus mobility to seasonal and diel redox fluctuations at the sediment–water interface in a eutrophic freshwater lake. Limnol. Oceanogr. 56, 2251–2264. http://dx.doi.org/10.4319/lo.2011.56.6.2251.
Søndergaard, M., Jensen, J.P., Jeppesen, E., 1999. Internal phosphorus loading in shallow Danish lakes. Hydrobiologia 408, 145–152.
Søndergaard, M., Jensen, J.P., Jeppesen, E., 2003. Role of sediment and internal loading of phosphorus in shallow lakes. Hydrobiologia 506, 135–145.
Søndergaard, M., Jensen, J.P., Jeppesen, E., 2005. Seasonal response of nutrients to reduced phosphorus loading in 12 Danish lakes. Freshw. Biol. 50, 1605–1615. http://dx.doi.org/10.1111/j.1365-2427.2005.01412.x.
Staehr, P.A., Testa, J.M., Kemp, W.M., Cole, J.J., Sand-Jensen, K., Smith, S.V., 2011. The metabolism of aquatic ecosystems: history, applications, and future challenges. Aquat. Sci. 74, 15–29. http://dx.doi.org/10.1007/s00027-011-0199-2.
Sterner, R.W., 2008. On the phosphorus limitation paradigm for lakes. Int. Rev. Hydrobiol. 93, 433–445. http://dx.doi.org/10.1002/iroh.200811068.
Sterner, R.W., Elser, J., 2002. Ecological Stoichiometry: the Biology of Elements From Molecules to the Biosphere. Princeton University Press.
Sterner, R.W., Elser, J.J., Fee, E.J., Guildford, S.J., Chrzanowski, T.H., 1997. The light: nutrient ratio in lakes: the balance of energy and materials affects ecosystem structure and process. Am. Nat. 150, 663–684. http://dx.doi.org/10.1086/286088.
Stumpf, R.P., Wynne, T.T., Baker, D.B., Fahnenstiel, G.L., 2012. Interannual variability of cyanobacterial blooms in Lake Erie. PLoS ONE 7, e42444. http://dx.doi.org/10.1371/journal.pone.0042444.t004.
Thomas, D.B., Schallenberg, M., 2008. Benthic shear stress gradient defines three mutually exclusive modes of non-biological internal nutrient loading in shallow lakes. Hydrobiologia 610, 1–11. http://dx.doi.org/10.1007/s10750-008-9417-x.
USEPA, 1993a. Method 353.2. Determination of Nitrate–Nitrite by Semi-automated Colorimetry Revision 2.0. United States Environmental Protection Agency.
USEPA, 1993b. Method 350.1. Determination of Ammonia Nitrogen by Semi-automated Colorimetry Revision 2.0. United States Environmental Protection Agency.
USEPA, 1993c. Method 365.1. Determination of Phosphorus by Semi-automated Colorimetry Revision 2.0. United States Environmental Protection Agency.
USEPA, 1995. Standard Method 4500-P E. Phosphorus: Ascorbic Acid Method, 19th Edition United States Environmental Protection Agency.
Van Luijn, F., Boers, P., Lijklema, L., Sweerts, J.-P., 1999. Nitrogen fluxes and processes in sandy and muddy sediments from a shallow eutrophic lake. Water Res. 33, 33–42.
Vanni, M.J., Andrews, J.S., Renwick, W.H., Gonzalez, M.J., Noble, S.J., 2006. Nutrient and light limitation of reservoir phytoplankton in relation to storm-mediated pulses in stream discharge. Fund. Appl. Limnol. 167, 421–445. http://dx.doi.org/10.1127/0003-9136/2006/0167-0421.
VTDEC (Vermont Department of Environmental Conservation), NYDEC (New York State Department of Environmental Conservation), 2014. Lake Champlain long-term water quality and biological monitoring program—Program description. Grand Isle, Vermont. http://www.watershedmanagement.vt.gov/lakes/htm/lp_longterm.htm.
Watzin, M.C., Fuller, S., May, C., Bronson, L., Rogalus, M., Linder, M., 2008. Monitoring and evaluation of cyanobacteria in Lake Champlain — summer 2007. Lake Champlain Basin Program. 56, 1–56.
Watzin, M., Fuller, S., Gorney, R., Caron, J., 2012. Monitoring and evaluation of cyanobacteria in Lake Champlain — 2011. Lake Champlain Basin Program. 71, 1–80.
Wehr, J.D., Sheath, R.G., 2002. Freshwater Algae of North America: Ecology and Classification. Academic Press.
Zamyadi, A., McQuaid, N., Prévost, M., Dorner, S., 2012. Monitoring of potentially toxic cyanobacteria using an online multi-probe in drinking water sources. J. Environ. Monit. 14, 579. http://dx.doi.org/10.1039/c1em10819k.